Dependence of the heavy-ion-induced desorption yield on the primary-ion energy loss

D. Brandl, Ch. Schoppmann, R. Schmidt, B. Nees, A. Ostrowski, and H. Voit
Physikalisches Institut der Universität Erlangen-Nürnberg, D-8520 Erlangen, Germany
(Received 5 June 1990; revised manuscript received 28 August 1990)

The dependence of the secondary-ion yield Y on the energy loss dE/dx of fast (MeV/u) primary ions has been measured for organic and inorganic samples. It is found that the dependence of Y on dE/dx can be expressed in the whole dE/dx range investigated ($1 \leq dE/dx \leq 54$ keV μg^{-1} cm^2) as $Y \propto (dE/dx - S)^n$, where S is a threshold energy loss. Different exponents n exist for positive and negative secondary ions as well as ions desorbed from different samples.

I. INTRODUCTION

It is well known from a great number of investigations performed to elucidate the mechanisms underlying the heavy-ion-induced desorption (HIID) that the electronic component of the primary-ion energy loss dE/dx is responsible for the desorption of neutral and charged particles from insulating materials (see Ref. 1 for a recent review). It is, therefore, quite natural to determine experimentally the dependence of the secondary-particle yield on the electronic stopping power of the MeV primary ions. Another obvious reason for these measurements is the fact that theoretical models[2,3] have been developed which predict the dependence of the yield on dE/dx.

Several authors have determined the yield both for neutral[4-6] and charged[4,7-10] particles as a function of dE/dx or, what is equivalent, as a function of the primary-ion energy and primary-ion velocity. Most of these measurements cover, however, only a very limited dE/dx range or do not contain enough data points to pin down the dE/dx dependence accurately. Therefore we have reinvestigated the dependence of the secondary-ion yield Y on dE/dx for a few inorganic and organic samples. The results are reported in this paper.

II. EXPERIMENTAL

The experimental setup is shown in Fig. 1. A low-intensity (a few hundred particles per second) beam of heavy ions (HI's) from the Erlangen EN tandem accelerator enters the vacuum chamber (10^{-6} Torr) from the right, penetrates a carbon foil F thick enough to establish charge state equilibrium, and hits the sample S with an angle $\theta = 30°$ with respect to the surface normal. Secondary ions (SI's) desorbed by the primary ions are analyzed by means of a time-of-flight (TOF) mass spectometer consisting of the field free flight path between the grids G1 and G2 (both at ground potential) and the ion detector. The secondary ions are accelerated in the electric field between S and G1, penetrate the flight path, hit the CsI-covered converter plate C (at -300 V), and produce secondary electrons which are accelerated between C and G2 and are bent by means of a magnetic field into the channel plate detector CP. This detector delivers the stop signal for the TOF measurement. The start signal is obtained from a surface barrier detector SB1 which registers the primary ions that have penetrated the sample. Start and stop signals are fed into a time digitizer which accepts 31 stop signals after one start event.

The secondary-ion yield was determined as the ratio between desorbed ions and the primary ions impinging upon the sample. All measured yields are relative yields because the detection efficiency of the TOF spectometer is not accurately known. The latter depends on the transmission of the grids, the geometry, and the efficiency of the channel plates which is known to depend on the velocity of the detected particles (the efficiency decreases with increasing mass of the particles). The efficiency of the detector used is estimated to be larger than 50% for particles with $m \approx 100$ u. All yields reported below can, however, be compared relative to each other since the measurements have been performed with identical experimental conditions in the same run.

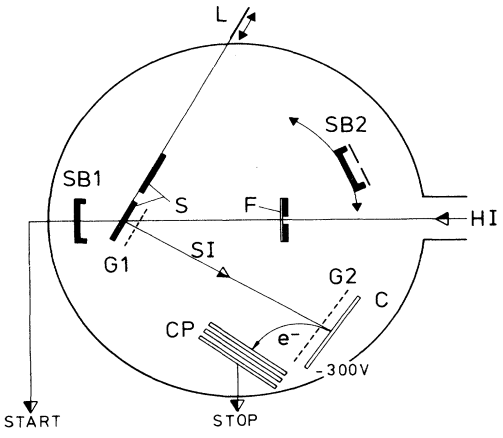

FIG. 1 Schematics of the experimental setup. HI and SI denote primary and secondary ions, respectively. F is a thin carbon foil mounted on a 2-mm (diameter) collimator. S are the samples (connected to ±9.3 kV) mounted on the movable ladder L, G1 and G2 are grids (on ground potential), and SB1 and SB2 are silicon detectors. C and CP denote the converter and the channel plate, respectively. For details see text.

TABLE I. Primary ions, primary-ion energies E, and velocities v used in the present investigations.

Primary ions	^{9}Be	^{12}C			^{16}O		^{28}Si		^{32}S	^{63}Cu
E (MeV)	11.65	26.5	15.0	24.25	15.6	10.55	50.01	25.25	25.05	58.4
v (cm ns^{-1})	1.57	2.06	1.55	1.71	1.39	1.12	1.85	1.32	1.23	1.33

Four different samples have been investigated consisting of (i) the inorganic salt CsI, (ii) the amino acid valine (M=117 u), and (iii) a biheterocyclic triphenylphosphoran[11] (sum formula $C_{48}H_{36}N_3O_2P$, abbreviated TPP in the following) with molecular mass 717 u and (iv) the saltlike compound tetrabutyl ammonium tetraphenyl borate. The latter is abbreviated as $(TBA)^+(TPB)^-$. The masses of the cation $(TBA)^+$ and the anion $(TPB)^-$ are 242 and 319 u, respectively.

The sample material was deposited by means of vacuum evaporation onto a thin Mylar foil covered by a 40-μg cm^{-2}-thick Au film. Only the TPP sample was prepared by means of the electrospray method. Sample thicknesses were of the order of 30 μg cm^{-2}. All samples were mounted on a movable target ladder (see Fig. 1) and were investigated one after the other without breaking vacuum.

The energy-loss values of a particular ion with energies obtainable from our accelerator cover only a limited range. In order to have, nevertheless, a broad dE/dx spectrum different primary ions with rather different dE/dx values were used for the present investigations. These primary ions are listed in Table I together with the ion energy E (at the smaple surface) and the ion velocity v.

The energy losses in the different samples were calculated from the Northcliffe-Schilling tables[12] by means of the Bragg-Kleeman relation.[13] For the case of the valine sample it was verified experimentally that the calculated stopping-power curve for ^{16}O ions is correct. This gives some confidence that the calculated dE/dx values for the remaining heavy ions are also reasonable. It should be noted that the primary-ion energies have been chosen in such a way that the corresponding dE/dx values lie on the right side of the Bragg maximum in the stopping-power curve (one exception is the dE/dx value for ^{63}Cu in CsI). This guarantees that the dE/dx ambiguity reported by Dück *et al.*[14] does not occur in the present data.

Due to possible sample inhomogeneities it is essential for the investigations that the sample is always hit at the same spot by the primary ions. In order to achieve this after a change to another heavy-ion beam special precautions were taken: a surface barrier detector (SB2, see Fig. 1) covered with a 2-mm collimator could be moved into the beam in order to optimize the beam through the small collimator in the carbon foil onto the sample surface. In addition a beam profile was also recorded.

III. RESULTS

Figure 2 shows spectra obtained with the 58.4-MeV ^{63}Cu beam from the TPP and $(TBA)^+(TPB)^-$ samples. The TPP spectrum clearly exhibits the protonated molecular ion $(M+H)^+$ and several fragment ions. The $(TBA)^+(TPB)^-$ spectra are dominated by the cation and anion peaks.

Yields of positive and negative ions desorbed from the valine sample are shown in Fig. 3 as a function of the energy loss of the primary ions. Obviously the shapes of the yield functions for positive ions are nearly identical. The same holds for the yield functions of negative ions. The latter are, however, considerably steeper than the yield functions of positive ions. It should be noted that the $(M+H)^+$ curve (M indicates the valine molecule) contains data points (solid circles) from a previous measurement.[10] Only those data points from Ref. 10 were inserted which are obtained for primary ions having roughly the same velocity (solid circles in Fig. 3, all other values would fit also into the remeasured curve). The previous data were obtained with an experimental method[15] which is superior to the method used in this work since it allowed us to measure secondary-ion yields as a function of dE/dx without changing the beam energy, i.e., without tuning the beam after each energy change. The agree-

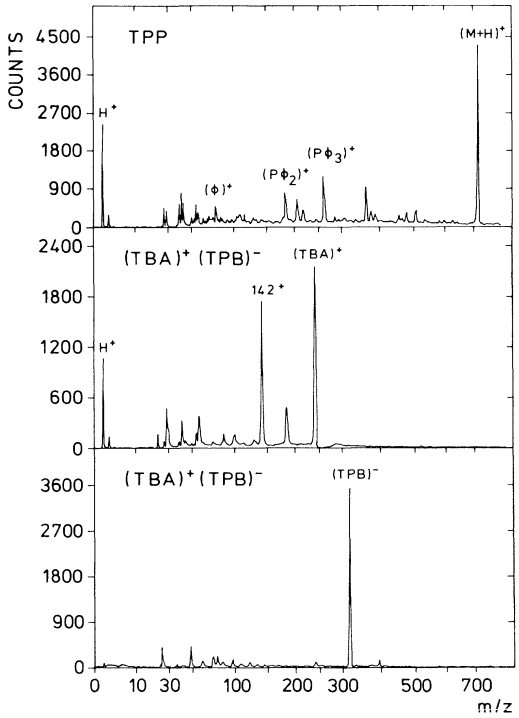

FIG. 2 TOF mass spectra obtained with 58.4-MeV ^{63}Cu primary ions from TPP (top) and $(TBA)^+(TPB)^-$ samples, respectively. M denotes the TPP molecule and ϕ^+ stands for C_6H_5.

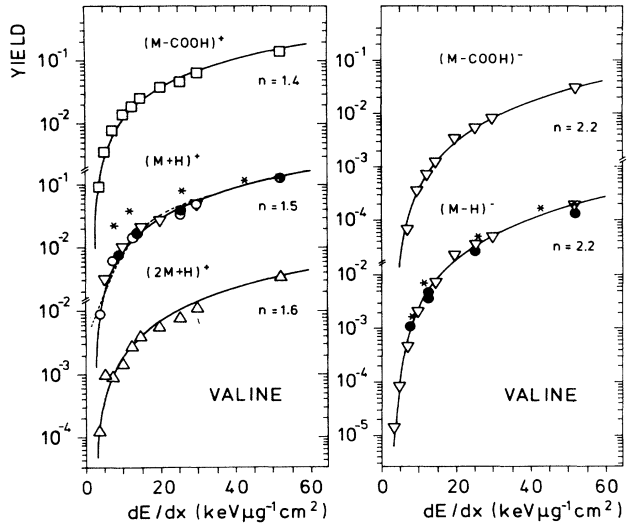

FIG. 3 Yield of positive and negative ions desorbed from a valine sample as a function of the primary-ion energy loss dE/dx. M denotes the valine molecule. The solid circles in the $(M+H)^+$ curve represent data points from previous measurements (Ref. 10). They are obtained with primary ions of the same velocity. The open circles mark data points from the present measurement obtained for primary ions with $v=1.39$ cm ns$^{-1}\pm 13\%$. Asteriks indicate yield functions for the protonated and deprotonated leucine molecules desorbed from a leucine sample [from Ref. 4, the data are normalized to our $(M+H)^+$ and $(M-H)^-$ data at the largest dE/dx value]. The solid lines represent the function $(dE/dx-S)^n$ with n values as indicated in the figure (S values are given in Table II). The dashed curve is the prediction of the ion track model for the $(M+H)^+$ ion calculated with $m=2$ (see Ref. 17).

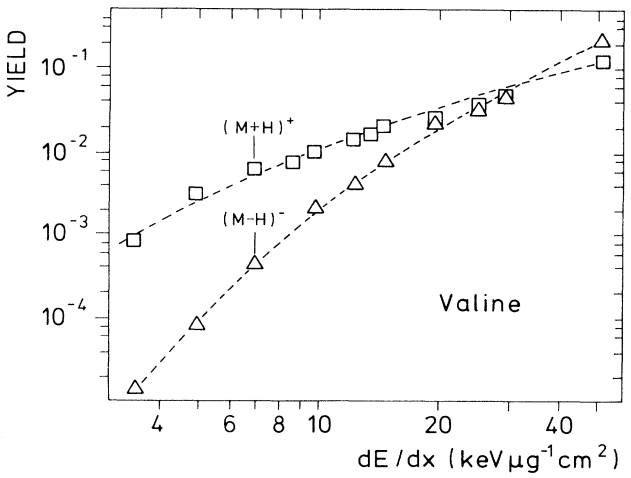

FIG. 4 Yield of $(M+H)^+$ and $(M-H)^-$ ions from a valine sample as a function of dE/dx. Dashed lines are guides for the eye.

ment between both data sets gives confidence that the present method (see Sec. II) gives reliable data.

It should be noted that primary ions with slightly different velocities v have been used in the present investigations in contrast to the measurements performed by the Uppsala group.[4,9] The motivation for a constant velocity comes from a model which assumes that an energy density proportional to dE/dx exists in a cylindrical shell surrounding the primary-ion track (inner and outer radius of the shell are proportional to v), and that the desorption occurs mainly from this shell and is proportional to the energy density. According to this model one would expect steps in the measured Y versus dE/dx curve if different primary ions with different velocities v are used as in the measurements of Refs. 7 and 10. This is, however, not the case; the measured Y dependences are continuous functions of dE/dx. This means that the model is either not correct or that the effects are too small to be visible within the experimental accuracy. Thus, it seems not to be necessary to use primary ions with the same velocity for this type of experiment (as long as the corresponding energies belong to the same branch of the electronic stopping-power curve). In fact, the data points of the present measurement obtained for primary ions with almost the same velocity ($v=1.39$cmns$^{-1}\pm 13\%$, marked by open circles in Fig. 3) and with velocities which differ considerably from the above value (triangles) give a continuous curve.

Figure 4 compares the $(M+H)^+$ and $(M-H)^-$ yields from the valine sample in a double logarithmic plot. Obviously the $(M-H)^-$ curve exhibits a steeper slope than the $(M+H)^+$ curve. Note that the data points do not fall on straight lines, indicating that the yields are not just proportional to $(dE/dx)^n$. Note also that the $(M-H)^-$ yield exceeds the $(M+H)^+$ yield for the largest dE/dx value measured.

The yield functions for positive and negative ions desorbed from the $(TBA)^+(TPB)^-$ sample are shown together with the data from the TPP sample in Fig. 5. The

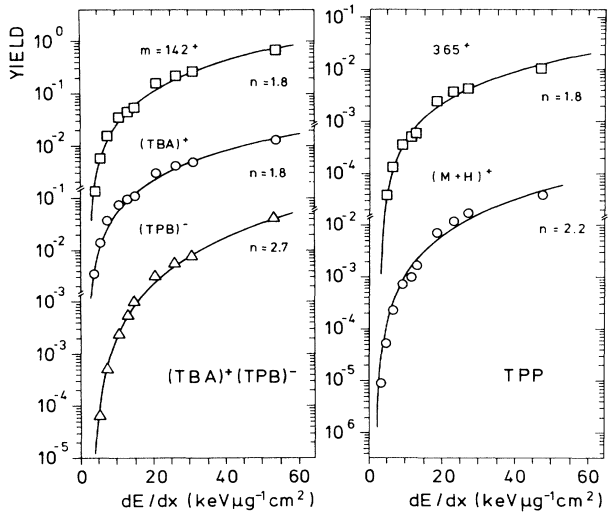

FIG. 5 Cation and anion yields from the $(TBA)^+(TPB)^-$ sample as well as the yield for $(M+H)^+$ ions desorbed from the TPP sample as a function of dE/dx. Also shown are the yield functions for the $m=142$ and 365 u fragment ions from the $(TBA)^+(TPB)^-$ and the TPP sample, respectively. For the solid lines see the caption for Fig. 3.

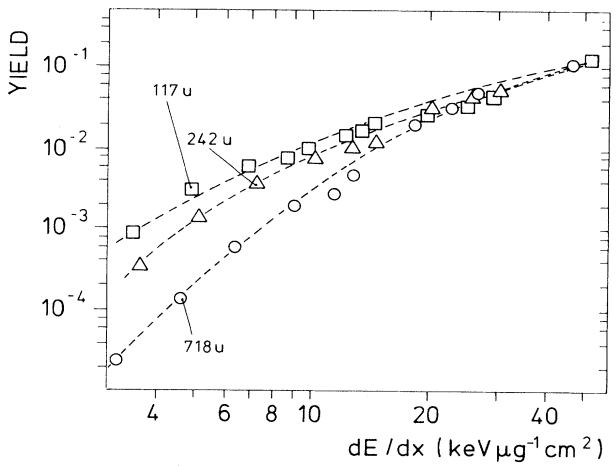

FIG. 6 Yield functions of the protonated valine ($m=117$ u) and TPP ($m=718$ u) molecule and of the $(TBA)^+$ ion ($m=242$ u). The data are normalized to each other at the largest dE/dx value. The dashed lines are guides for the eye.

cation $(TBA)^+$ ($m=242$ u) and the fragment ion with mass $m=142$ u have identical yield functions with a slope which is less steep than that of the $(TPB)^-$ anion ($m=319$ u). The yield function of the protonated TPP molecular ion ($m=718$ u) exhibits a steeper slope than the yield function of the lighter (or smaller) fragment ion ($m=365$ u). This trend can also be seen from Fig. 6 in which the yield functions for the positive parent ions from all organic samples investigated are shown. The latter is also obvious from Fig. 7, which shows the $(TBA)^+$ and $(TPB)^-$ yields in a log-log plot. It is interesting to note that the $(TBA)^+$ yield of this organic salt exceeds the $(TPB)^-$ yield over the whole dE/dx range.

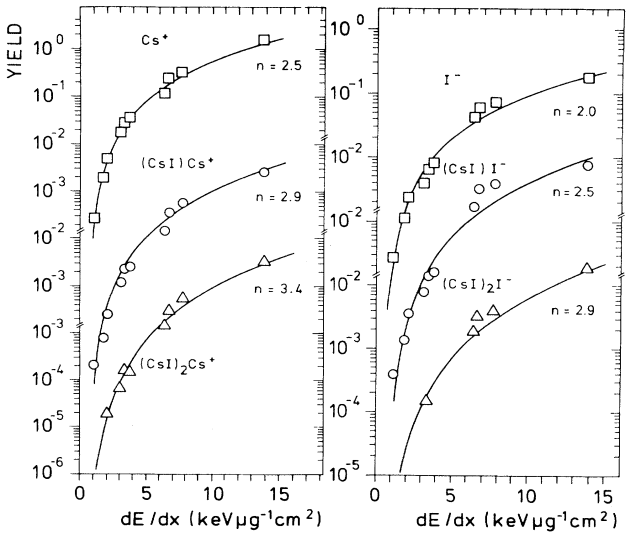

FIG. 7 Yield functions for $(CsI)_nCs^+$ and $(CsI)_nI^-$ ions ($n=0-2$) desorbed from a CsI sample. For the solid lines see the caption for Fig. 3.

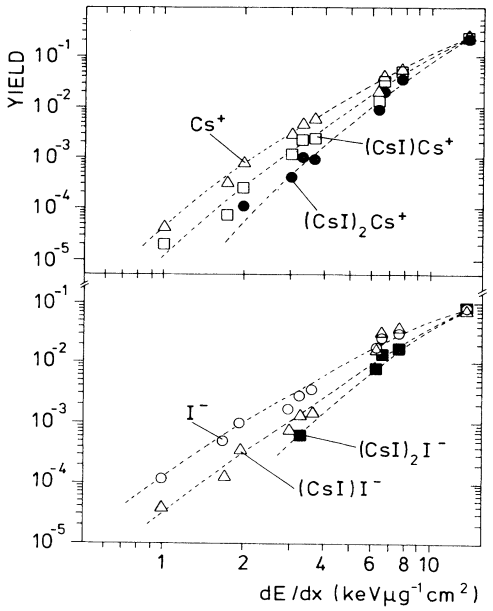

FIG. 8 Yield functions for $(CsI)_nCs^+$ and $(CsI)_nI^-$ ions ($n=0-2$) normalized to each other at the largest dE/dx value. Dashed lines are guides for the eye.

An increase of the slope of the yield function with increasing mass of the desorbed ion is also observed in Fig. 7, which displays the yields of $(CsI)_nCs^+$ and $(CsI)_nI^-$ ions ($n=0-2$) desorbed from the CsI sample. This behavior is even more pronounced in the double logarithmic plot of Fig. 8. In addition it is interesting to note that the I^- yield equals the Cs^+ yield at the smallest dE/dx values investigated (see Fig. 9). It increases, however, less rapidly with increasing dE/dx than the Cs^+ yield. A similar behavior exists for the $(CsI)_nI^-$ yields compared with the $(CsI)_nCs^+$ yields.

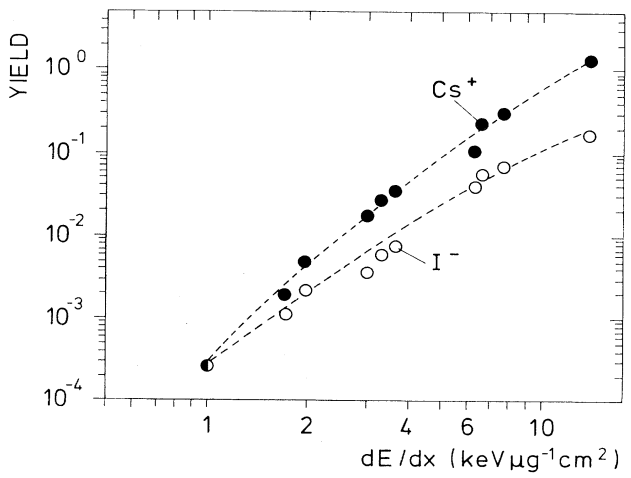

FIG. 9 Yield functions for Cs^+ and I^- ions. Note that the Cs^+ and I^- yields are identical for the smallest dE/dx values. Dashed lines are guides for the eye.

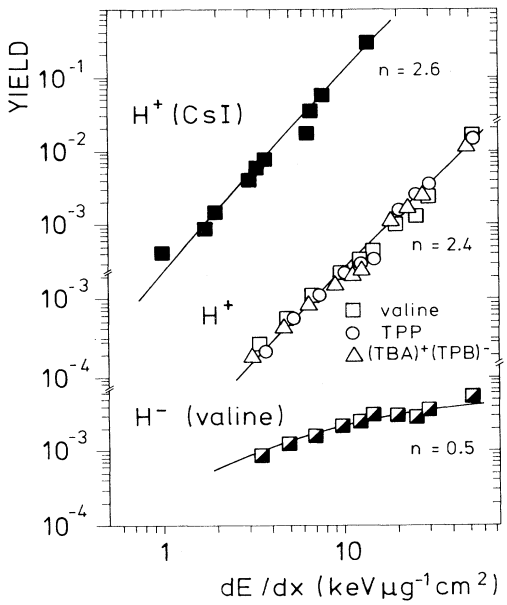

FIG. 10 Yield functions for H^+ and H^- ions desorbed from different samples. For the solid lines see the caption for Fig. 3.

Figure 10 shows the H^+ yields obtained for all samples investigated as well as the H^- yield from the valine sample. The H^+ yields from the organic samples have the same absolute values and the same dependence on dE/dx. On the contrary, the H^+ yield from the CsI sample is roughly one order of magnitude larger than the H^+ yield obtained for similar dE/dx values from organic samples. In addition the dE/dx dependence is more pronounced for H^+ ions from the CsI sample compared with the H^+ yields from the organic samples. The same results are obtained for Na^+ and C_2H^- ions desorbed from the organic samples and the CsI sample, respectively.

IV. DISCUSSION

All yield functions measured in this work can be reproduced within the dE/dx range investigated (1–54 keV μg^{-1} cm^2) by the following expression:

$$Y = A\,(dE/dx - S)^n \tag{1}$$

with A being a normalization constant (which is zero for $dE/dx < S$) and S a threshold value for the primary-ion energy loss dE/dx. Apparently a secondary ion can only be desorbed if dE/dx exceeds the threshold S specific for this particular ion. The existence of a desorption threshold seems to be quite natural. Dück[16] has found already in an early investigation of the dependence of the secondary-ion yield on dE/dx that such a threshold exists: no sample-specific ions could be desorbed from a valine sample by α particles ($dE/dx \approx 1.5$ keV μg^{-1} cm^2). The existence of the threshold S is most clearly demonstrated in the double logarithmic plots: the data points do not fall on a straight line.

The solid lines in the previous figures represent fits to the experimental data obtained with Eq. (1). The fit parameters S and N are given in Table II. It should be not-

TABLE II. Threshold value S and exponent n used to fit the experimental yield curves with equation $Y \propto (dE/dx - S)^n$.

Sample	Secondary ion	m (u)	S (keV μg^{-1} cm^2)	n
	$(M-COOH)^+$	72	2.0	1.4
	$(M+H)^+$	118	2.0	1.5
	$(2M+H)^+$	235	2.0	1.6
Valine	$(M-COOH)^-$	72	3.5	2.2
	$(M-H)^-$	116	3.5	2.2
	H^+	1	0.2	2.4
	Na^+	23	0.1	1.9
	H^-	1	2.5	0.51
	$m=142$	142	1.6	1.8
	$(TBA)^+$	242	1.6	1.8
$(TBA)^+(TPB)^-$	$(TPB)^-$	319	2.8	2.7
	H^+	1	0.2	2.4
	$m=365$	365	3.0	1.8
TPP	$(M+H)^+$	718	1.7	2.2
	H^+	1	0.2	2.4
	Cs^+	133	0.6	2.5
	$(CsI)Cs^+$	393	0.6	2.9
	$(CsI)_2Cs^+$	653	0.6	3.4
CsI	I^-	127	0.6	2.0
	$(CsI)I^-$	387	0.6	2.5
	$(CsI)_2I^-$	647	0.6	2.9
	H^+	1	0.1	2.6

ed that the quality of the fits does not change significantly if n and S values are used which differ from the values of Table II by typically 10% and 40%, respectively.

Several general trends can be deduced from Table II: (i) The yield increases the more rapidly with increasing dE/dx the heavier (or larger) the secondary ion is (i.e., the exponent n increases with mass m of the desorbed molecular ion), (ii) the yield of negative ions desorbed from *organic* samples depends more strongly on dE/dx than the yield of positive ions (the exponent n for negative ions exceeds that for positive ions), (iii) the threshold S for negative *organic* ions is larger than that for positive organic ions, and (iv) the thresholds for positive molecular ions from all three organic samples investigated are comparable.

The results obtained for the inorganic sample CsI differ from those for the organic samples in points (ii) and (iii). We find instead of (ii) that the exponent n for negative ions is smaller than that of positive ions with comparable mass, and instead of (iii) that the threshold values S are comparable for all sample-specific secondary ions.

Most of these trends have been observed already by the experimental groups working in the field of HIID. Hakansson *et al.*[9] were the first to realize that the exponent n increases with increasing mass and size of the secondary ion [point (i)]. This observation was a stimulus for the developement of the ion track model.[17] Figure 3 contains a comparison between the prediction of this model and the data for $(M+H)^+$ ions desorbed from the valine sample.

Instead of the ideas entering into the track model one could adopt a simple geometric explanation for the increase of n with m The primary ion mills a conical crater into the sample the depth and width of which increases with increasing dE/dx. Intact secondary particles emerge from the volume of this crater with the exception of a small cylinder with very high energy density surrounding the primary-ion track in which fragmentations occur. One can easily imagine that the remaining desorption volume of the crater increases with dE/dx much faster for extended than for smaller molecules if both crater and large molecule have comparable dimensions. This means indeed that the observed increase of n with increasing mass is rather due to the increase of the molecular size. Crater formation[18,19] in organic samples as well as the increase of the crater depth and width with increasing primary-ion energy loss[20] seems to be established from recent experiments with Langmuir-Blodgett films.

The fact that the yield of negative ions from organic samples increases much faster with dE/dx than the yield of positive ions [point (ii)] has been observed already in an early investigation of Nees *et al.*[21] (see also Ref. 7). An equally important observation is that the yields for positive ions from organic samples exceed the yields for negative ions at the smallest dE/dx values investigated. The yield differences for positive and negative ions decrease, however, with increasing dE/dx due to the much steeper slope of the yield function for negative ions. In case of the valine sample we even observe that the $(M-H)^-$ yield starts to surpass the $(M+H)^+$ yield at the largest dE/dx values (see Fig. 4). These observations are in contrast to the results obtained for the CsI sample: Cs^+ and I^- yields are equal at the smallest dE/dx values studied, the Cs^+ yield increases faster with increasing dE/dx than the I^- yield, with the result that the latter is roughly a factor of 10 smaller than the Cs^+ yield at the highest dE/dx value investigated (see Fig. 10).

Equal yields for Cs^+ and I^- ions are what one expects intuitively for an inorganic salt sample like CsI consisting of microcrystallites containing preformed cations and anions. At small dE/dx values mostly electronic excitations of the ions close to the primary-ion track occur which are partly deexcitated without radiative transitions. Part of the energy loss is thus converted into phonons which in turn transfer kinetic energy to the Cs^+ and I^- ions, which subsequently escape with equal intensity. With increasing dE/dx electrons are removed from the ions close to the primary-ion trajectory. Mostly I^- ions are affected, i.e., neutralized, due to the small value of the electron affinity (compared with the $5p$ excitation energy in Cs^+). The Cs^+ ions close to the trajectory experience thus a strong repulsion and effuse into the vacuum from a crater the volume of which increases with increasing dE/dx. I^- ions stem mainly from regions far apart from the heavy-ion trajectory (the distance from the trajectory is larger than the maximum impact parameter of the Bohr theory[22] for the energy loss of fast charged particles in matter) at these elevated dE/dx values. As a result of these mechanisms the Cs^+ yield increases more rapidly with increasing dE/dx than the I^- yield; besides this, one expects the same threshold values S for the Cs^+ and I^- yields in this picture.

The different behavior of the cation and anion yields from the inorganic salt $(TBA)^+(TPB)^-$ shown in Fig. 11 are explainable if one assumes (i) that all ions within a cylindrical volume around the primary-ion path become fragmented due to the high energy density in this volume and (ii) that the dependence of the yield on dE/dx is more pronounced for the more extended $(TPB)^-$ molecules than for the $(TBA)^+$ molecules desorbed from a conical crater centered around the above-mentioned cylindrical volume. The existence of a fragmentation re-

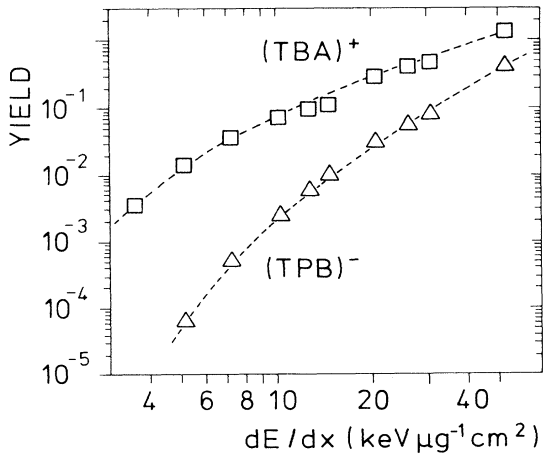

FIG. 11 Cation and anion yields from the $(TBA)^+(TPB)^-$ sample as a function of dE/dx. The dashed lines are guides for the eye.

gion prevents the Coulomb repulsion from becoming as effective for $(TBA)^+$ ions as in the Cs^+ case. Thus one expects that the $(TBA)^+$ yield exceeds the $(TPB)^-$ yield significantly at small dE/dx values and that the difference between $(TBA)^+$ and $(TPB)^-$ yields decreases with increasing crater volume, i.e., with increasing dE/dx.

$(M+H)^+$ and $(M-H)^-$ ions desorbed from the valine sample are most probably not preformed as is the case for CsI and $(TBA)^+(TPB)^-$. The valine sample represents an amorphous aggregation of molecules interconnected mainly by hydrogen bonds. The $(M+H)^+$ ion does not originate in a one-step desorption process in which a proton from a neighbor molecule remains at the molecule after bond breaking. The reason is that the strength of the hydrogen bond is significantly smaller than the intramolecular binding of the hydrogen. Moreover, if the one-step desorption process would contribute considerably, one would expect similar yields for $(M+H)^+$ and $(M+H)^-$ ions for all dE/dx values.

The $(M+H)^+$ ion rather originates from a two-step desorption process in which a proton is transferred onto a neutral valine molecule M^0 which has already gained kinetic energy. The protons stem either from hydrogen contamination of the sample or from fragments generated in the fragmentation zone. The M^0 yield exceeds the $(M+H)^+$ yield by several orders of magnitude.[4,6] This guarantees reasonable yields for $(M+H)^+$ in a two-step process. The cross section for the intermolecular proton transfer is expected to decrease with increasing dE/dx, whereas both the M^0 and the H^+ flux is expected to increase.

$(M-H)^-$ ions are assumed to result from internally excited M^0 molecules which deexcite via proton emission. Since the excitation probability is rather small for small dE/dx values we expect also a small $(M-H)^-$ yield for small energy losses. Moreover, a larger dE/dx threshold S for $(M-H)^-$ ions compared to $(M+H)^+$ ions seems to be reasonable (see Table II). With increasing dE/dx both the M^0 production and the degree of internal excitation increase rapidly. One thus expects a steep increase of the $(M-H)^-$ yield. This increase with dE/dx exceeds that of the $(M+H)^+$ production because two processes are involved in the latter, which hinder the $(M+H)^+$ formation with increasing dE/dx (decreasing proton transfer cross section and cleavage of protons due to the deexcitation of internally excited valine molecules).

It should be noted that other processes like fragmentation of larger clusters or one-step desorption processes may contribute to the $(M+H)^+$ and $(M-H)^-$ production. They seem, however, not to be the leading processes in the case of the valine sample.

As mentioned already, we observe comparable thresholds S for the desorption of positive ions from organic samples [point (iv)]. Due to the large uncertainty involved in the determination of the S values it is, however, not clear if this observation is really of significance. It should be pointed out, however, that comparable S and n values for fragment and parent ions desorbed from the valine and $(TBA)^+(TPB)^-$ samples most probably indicate that the fragment ions stem from the decay of the parent ions.

A comparison of the present experimental data with other data from organic or alkali halide samples measured in a comparable large dE/dx range is only possible for our early measurements performed for a valine sample[7,10] and for measurements performed by the Uppsala group.[4,9,23] Our previous $(M+H)^+$ and $(M-H)^-$ data for a valine sample fit nicely into the present yield functions (see Fig. 3). A comparison between our data for $(M+H)^+$ and $(M-H)^-$ ions desorbed from the valine sample and the Uppsala data for $(M+H)^+$ and $(M-H)^-$ ions from a leucine sample (both samples are amino acids) is given in Fig. 3.

In Ref. 9 it is stated that there is no simple scaling for the yield with dE/dx in the whole energy-loss range. This conclusion cannot be drawn from our present yield functions, which all can be reproduced by Eq. (1). In Ref. 4, on the other hand, it is claimed that the $(M+H)^+$ and $(M-H)^-$ yields from a leucine sample scale with $(dE/dx)^1$ and $(dE/dx)^2$, respectively. We would expect that the amino acid leucine should give the same results as the valine sample because identical yield functions were observed for a number of amino acids (in a smaller dE/dx interval) in Ref. 7. In fact, the $(M+H)^+$ data of experiment 2 in Ref. 4 can be reasonably reproduced by Eq. (1) with $S=2.0$ keV$\mu\,g^{-1}\,cm^2$ and $n=1.3$. Simiarly the $(M-H)^-$ data can be fitted with $S=3.5$ keV$\,\mu g^{-1}\,cm^2$ and $n=2.2$.

V. CONCLUSION

Secondary-ion yields measured as a function of the primary-ion energy loss dE/dx reveal rich information concerning the mechanisms underlying the desorption process. Of particular importance is a comparison of the relative yields and the dE/dx dependence for positive and negative parent ions desorbed from a particular sample, since it allows us to draw conclusions concerning the desorption processes involved.

All yield functions measured scale with $(dE/dx-S)^n$ where S is an energy-loss threshold which must be overcome to allow desorption of a particular species. The exponent n does not have a universal value, it has different values for different samples and secondary ions with comparable size. Generally an increase of n is observed for an increase of the size of the desorbed species. The exponent n for negative ions exceeds that of positive ions desorbed from organic samples, in contrast to the finding for the alkali halide sample CsI where $N(Cs^+)>N(I^-)$ is observed.

[1]K. Wien, Radiat. Eff. Def. Solids **109**, 137 (1989).

[2]R. E. Johnson, Int. J. Mass Spectrom. Ion Proc. **78**, 357 (1987).

[3]I. S. Bitensky, A. M. Goldenberg, and E. S. Parilis, in *Proceedings of the Fifth International Conference on Ion Formation from Organic Solids (IFOS V)*, Lövanger, Sweden, 1989, edited by A. Hedin, B. U. R. Sundqvist, and A. Benninghoven (Wiley, Chichester, 1990), p. 205.

[4]A. Hedin, P. Hakansson, M. Salehpour, and

B. U. R. Sundqvist, Phys. Rev. B **35**, 7377 (1987).
[5]W. Guthier, in *Proceedings of the Third International Workshop on Ion Formation from Organic Solids,* Münster, Federal Republic of Germany, 1985, edited by A. Benninghoven [Springer Proc. Phys. **9**, 17 (1986)].
[6]B. Nees, Ph.D. thesis, University of Erlangen-Nürnberg, 1988 (unpublished).
[7]E. Nieschler, B. Nees, H. Voit, P. Beining, and J. Scheer, Phys. Rev. B **37**, 9197 (1988); **38**, 8640 (1988).
[8]O. Becker, S. Della-Negra, Y. LeBeyec, and K. Wien, Nucl. Instrum. Methods Phys. Res. B **16**, 321 (1986).
[9]P. Hakansson, I. Kamensky, M. Salehpour, B. Sundqvist, and S. Widdiyasekera, Radiat. Eff. **80**, 141 (1984).
[10]H. Voit, E. Nieschler, B. Nees, R. Schmidt, Ch. Schoppmann, P. Beining, and J. Scheer, J. Phys. (Paris) C **2**, 237 (1989).
[11]H. J. Bestmann, Angew. Chem. **89**, 361 (1977).
[12]L. C. Northcliffe and K. F. Schilling, Nucl. Data Tables A **7**, 233 (1970).
[13]W. H. Bragg and R. Kleeman, Philos. Mag. **10**, 5318 (1905).
[14]P. Dück, H. Fröhlich, W. Treu, and H. Voit, Nucl. Instrum. Methods **168**, 601 (1980).
[15]P. Dück, H. Fröhlich, W. Treu, and H. Voit, Nucl. Instrum. Methods **189**, 615 (1981).
[16]P. Dück, Ph.D. thesis, University Erlangen-Nürnberg, 1981 (unpublished).
[17]A. Hedin, P. Hakansson, B. Sundqvist, and R. E. Johnson, Phys. Rev. B **31**, 1780 (1985).
[18]G. Bolbach, S. Della-Negra, C. Deprun, Y. LeBeyec, and K. G. Standing, Rapid Commun. Mass Spectrom. **1**, 22 (1987).
[19]G. Säve, P. Hakansson, B. U. R. Sundqvist, R. E. Johnson, E. Söderström, S. E. Lindqvist, and J. Berg, Appl. Phys. Lett. **51**, 1379 (1987).
[20]R. Schmidt, Ch. Schoppmann, D. Brandl, A. Ostrowski, and H. Voit (unpublished).
[21]B. Nees, E. Nieschler, N. Bischof, P. Dück, H. Fröhlich, W. Tiereth, and H. Voit, Radiat. Eff. **77**, 89 (1983).
[22]N. Bohr, Philos. Mag. **25**, 10 (1913).
[23]P. Hakansson and B. Sundqvist, Radiat. Eff. **61**, 179 (1982).